Searching for sand reservoirs: Processing 3C-3D seismic data from Manitou Lake, Saskatchewan

Han-xing Lu, Kevin W. Hall, Robert R. Stewart, D. Feuchtwanger[1] and Bryan Szatkowski[2]

ABSTRACT

In February 2005, a 3C-3D seismic survey was acquired by Kinetex Inc. for Calroc Energy Inc. near Manitou Lake, Saskatchewan. Exploration targets of the survey include oil and gas in the Colony sand member and the Sparky Formation of the Lower-Cretaceous Mannville Group. Reflections are observed throughout the vertical component shots, but are not as prominent on the radial component. The dominant frequency of the *P-P* data is about 75 Hz, while that of the *P-S* data is approximately 50 Hz. The final migrated *P-P* and preliminary migrated *P-S* volumes both have good reflectivity and tie well to synthetic seismograms. *P-P* time-slices show an amplitude anomaly that is interpreted to be a Colony sand channel. The preliminary *P-S* sections correlate reasonably well with the *P-P* sections. Following completion of radial component processing, these data will be good candidates for litholology interpretation and fluid estimation.

INTRODUCTION

In February 2005, a 3C-3D seismic survey was acquired by Kinetex Inc. for Calroc Energy Inc. near Manitou Lake, Saskatchewan. Production in this area include oil from the Colony sand member and Sparky Formation (sandstone) of the Lower Cretaceous Mannville Group. The Colony sand is the most recent member of the upper Mannville Group, which is a series of anastomosing sand channels, separated from each other by siltstones, shales, and thin sandstones, and is unconformably overlain by the Joli Fou Formation shales (Putnam and Oliver, 1980). The multiple channels may contain gas, oil and/or brine. Ideal reservoirs are structurally high (above the water contact). Seismic interpretations of the Colony sand has previously been reported for a different survey by Royle (2001; ibid 2002). We have re-processed the vertical component (*P-P*) data and are currently processing the radial component (*P-S*) volume.

[1] Aguila Exploration Consultants Ltd., Calgary, Alberta
[2] Calroc Energy Ltd.., Lloydminster, Alberta

FIG. 1. Location of the Manitou Lake 3C-3D seismic survey.

Acquisition

The survey covered approximately 10 km^2. Twenty-one south-north receiver lines and eighteen west-east source lines with 200 m line spacing and 50 m station spacing were acquired, for a total of 1072 source points and 1060 receiver locations (Figure 2). CDP and ACP fold (assuming V_P/V_S = 2.3) for 50x50 m bins are shown in Figure 3. Acquisition parameters are shown in Table 1.

Table 1. Acquisition parameters (Kinetex Inc.).

Recording System	I/O System 4
Source	Two vertical vibrators (IVI Y2400)
Source Array	16 m dragged array, 8 sweeps per VP, 1.14 m move-up per sweep. Diversity stacked in the field.
Sweep	8-144 Hz over 10 s with 5 s listen time
Receiver	I/O VectorSeis SVSM
Receiver Array	Single sensor per station
Station spacing	50 m source and receiver station spacing
Line spacing	200 m source and receiver line interval
Receiver lines	21 lines, total length 51.93 km
Source lines	18 lines, total length 53.89 km
Total area	~10 km^2

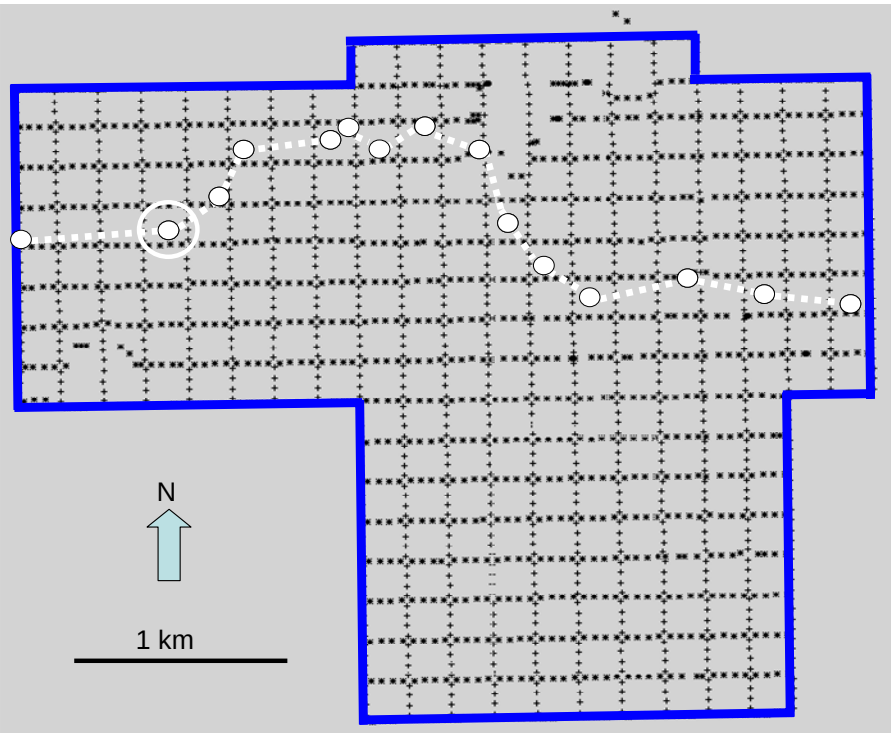

FIG. 2. Manitou Lake base map. Receiver lines are west-east, source lines are north-south. Dashed line and circles (white) show wells that follow a Colony sand member channel. The circled well location is 11-17.

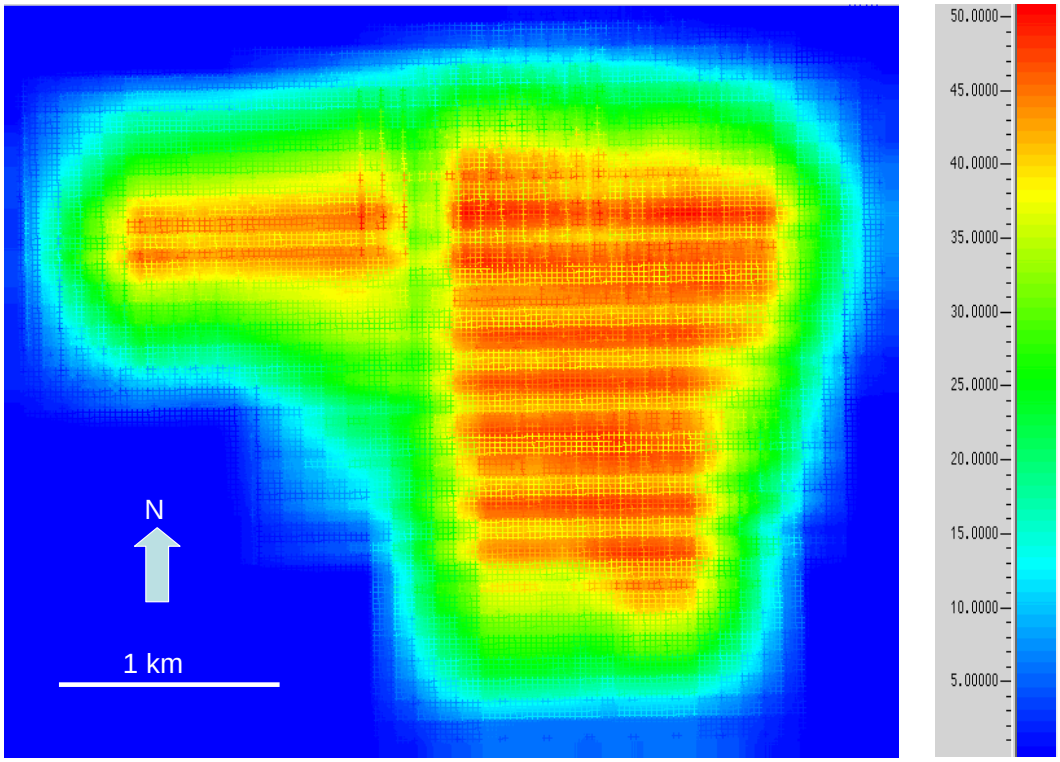

FIG. 3a. CDP fold for 50x50 m bin size. The maximum fold is ~50.

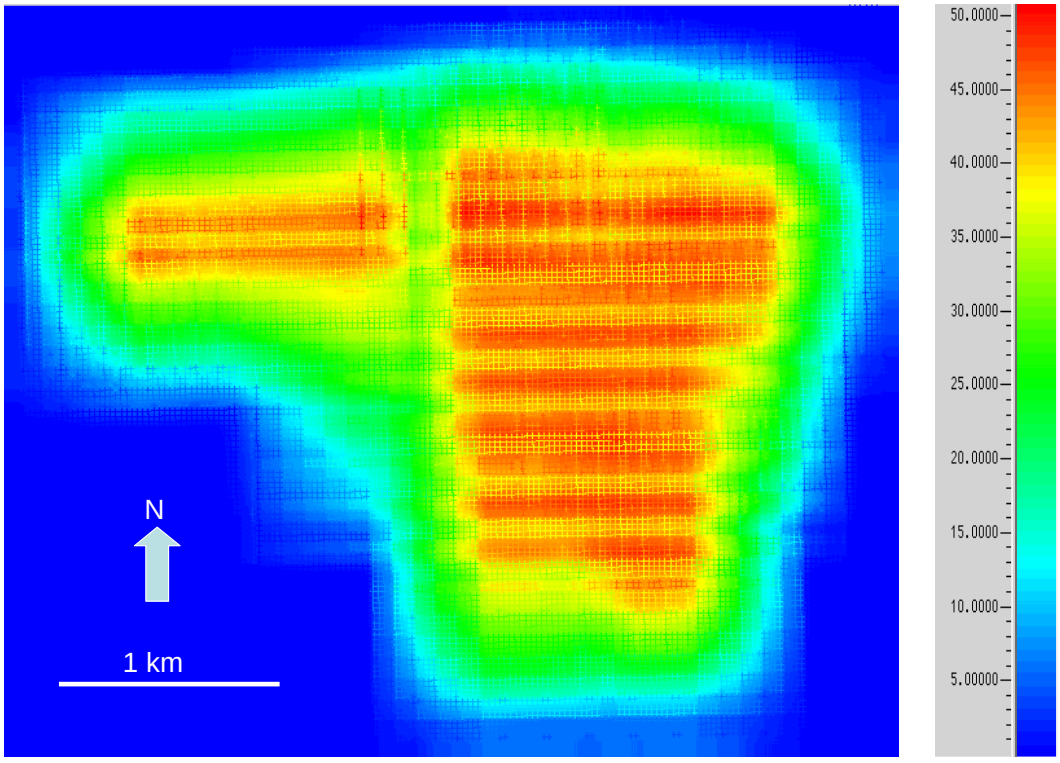

FIG. 3b. Converted-wave fold for 50x50 m bin size assuming V_P/V_S = 2.3. The maximum fold is ~70.

RESULTS

The vertical (*P-P*) component data has been processed to a final migrated volume, and work on the radial (*P-S*) component data is in progress. Conventional processing flows have been employed, as described by Lu and Margrave (1998) and detailed by Lu and Hall (2003).

Signal content

Examples of raw vertical and *P-S* radial shot gathers (Figure 4), and their corresponding amplitude spectra (Figure 5) show frequency content over a similar range as the sweep (12-144 Hz vs. 8-144 Hz). Most of the coherent energy is in the 18-75 Hz range for this survey. The *P-P* shot gathers show good reflectivity throughout (Figure 5a). However, the *P-S* shot gathers are significantly noisier, and at first blush, have the most reflectivity in a band between 1.4-1.6 seconds. These shot gathers also contain large amounts of spatially aliased noise (Figure 6). Interestingly, the amplitude spectra obtained from the vertical and radial component shot gathers are practically identical – implying that the digital geophones have the same frequency response regardless of orientation (and may be recording similar noise).

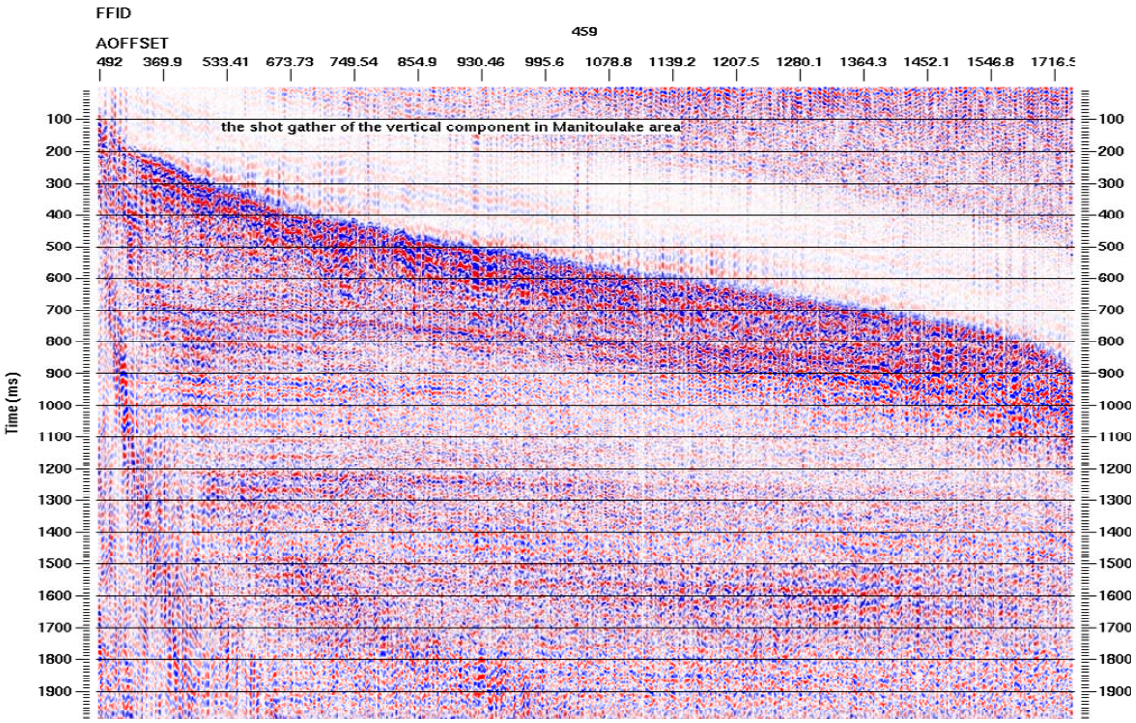

FIG. 4a. Vertical component shot gather sorted by absolute value of source-receiver offset.

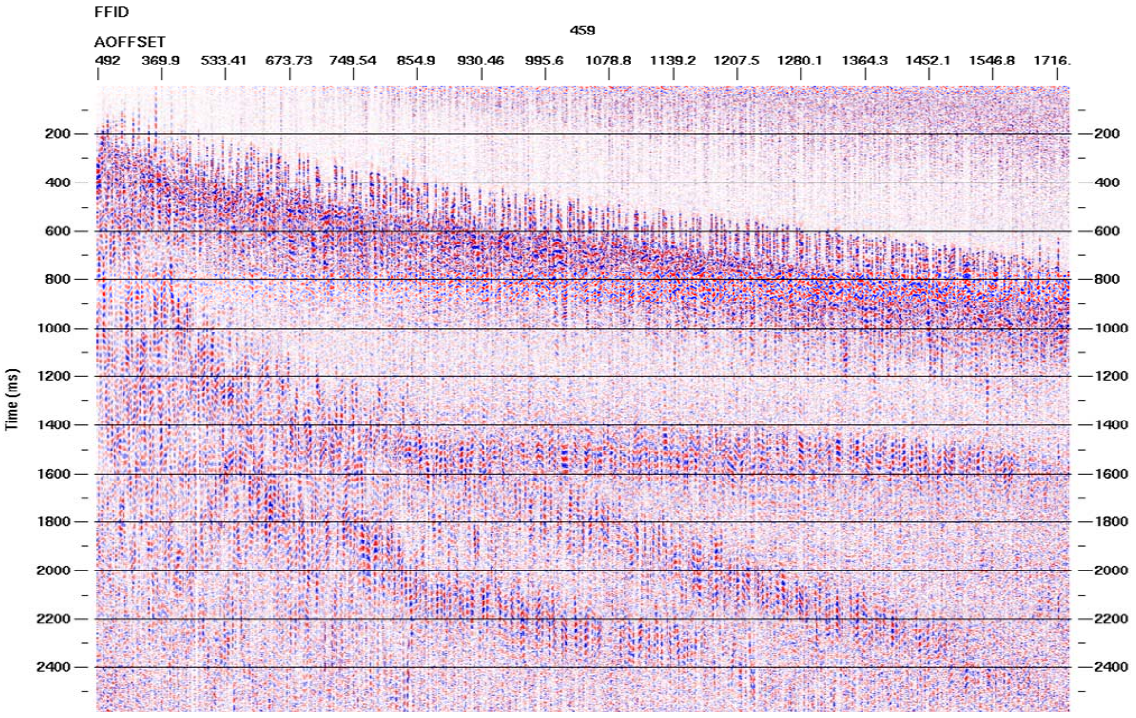

FIG. 4b. Radial component shot gather sorted by absolute value of source-receiver offset.

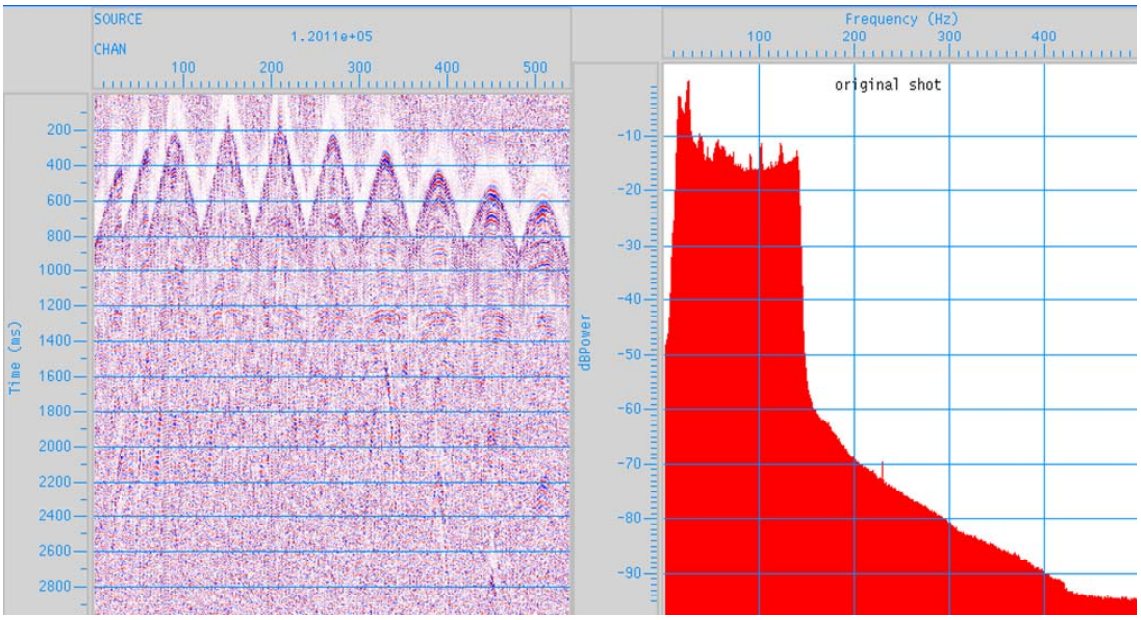

FIG. 5a. Amplitude spectrum for a vertical component shot gather (Same data as Figure 4a).

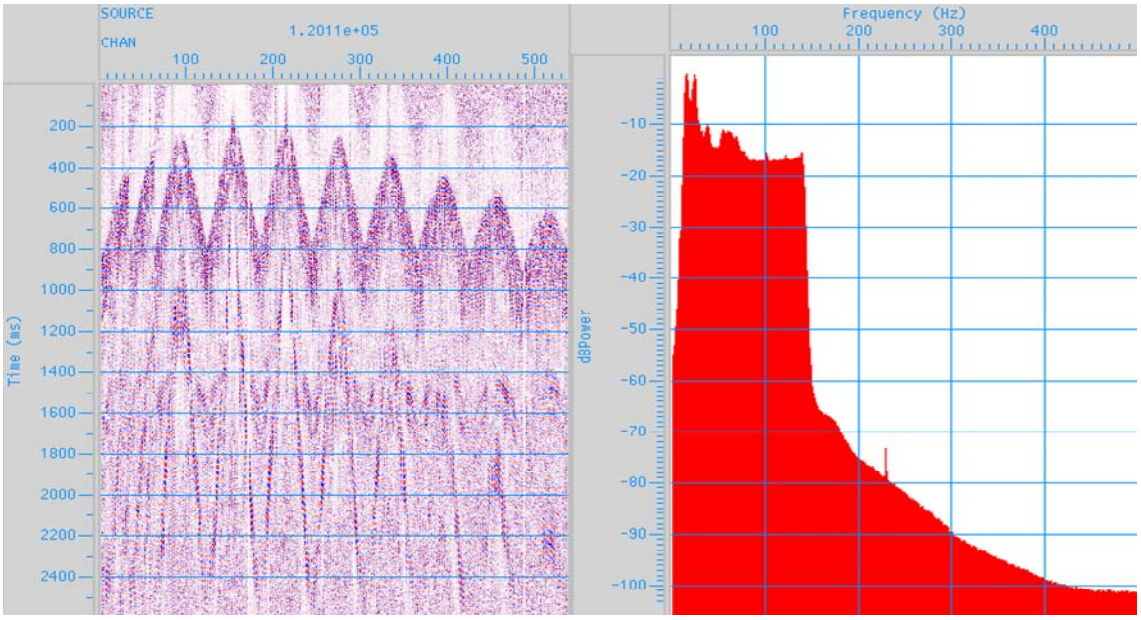

FIG. 5b. Amplitude spectrum for a radial component shot gather (Same data as Figure 4b).

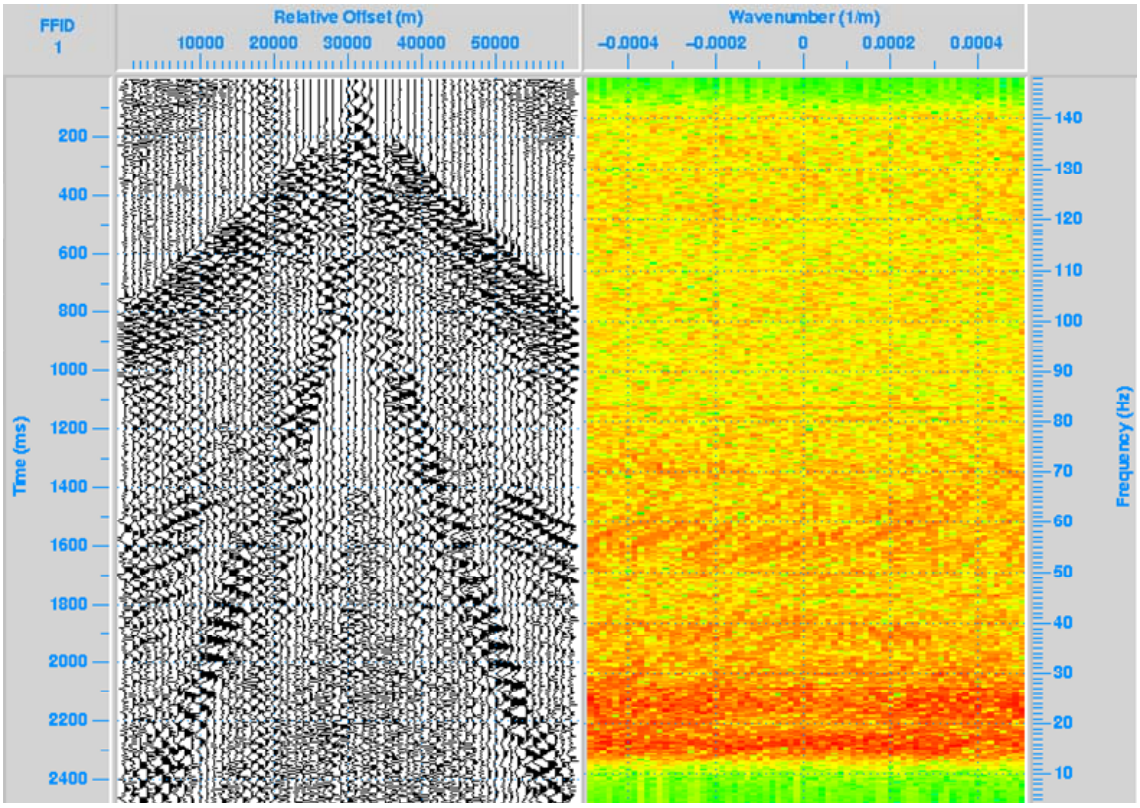

FIG. 6. Portion of a radial component shot gather (left) and *f-k* analysis (right).

Velocity analysis

Figure 7 shows an example of semblance-based velocity analysis for a *P-P* CDP super-gather and a *P-S* ACP super-gather. The horizontal velocity (left) and offset (right) scales are for Figures 7a and 7b. The *P-S* time scale in Figure 7b has been stretched to ~*P-P* time. In general, the picked velocity functions follow the same trend, with lower velocities between 300-750 ms and 800-1200 ms (*P-P* and *P-S* respectively). The *P-S* data are much noisier than the vertical, and velocities are correspondingly more difficult to pick. Near-offsets (0-400 m) have been excluded in order to reduce the effects of source noise for Figure 7b.

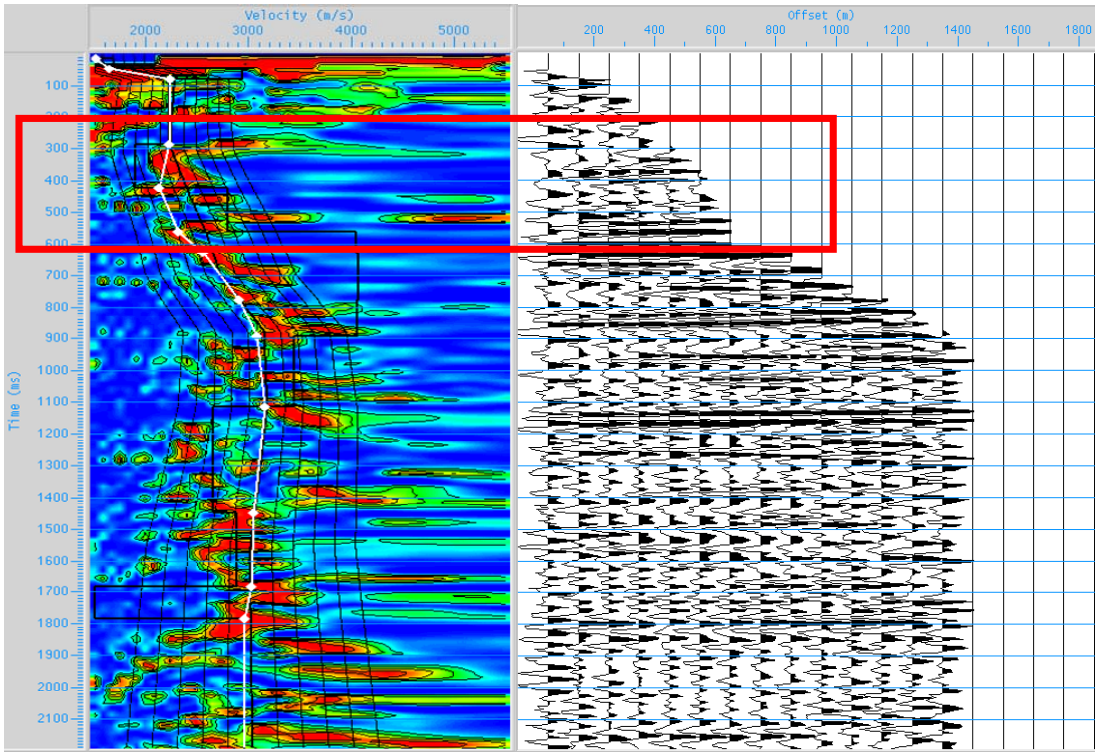

FIG. 7a. Vertical component semblance-based velocity analysis. Super-CDP gather is on the left.

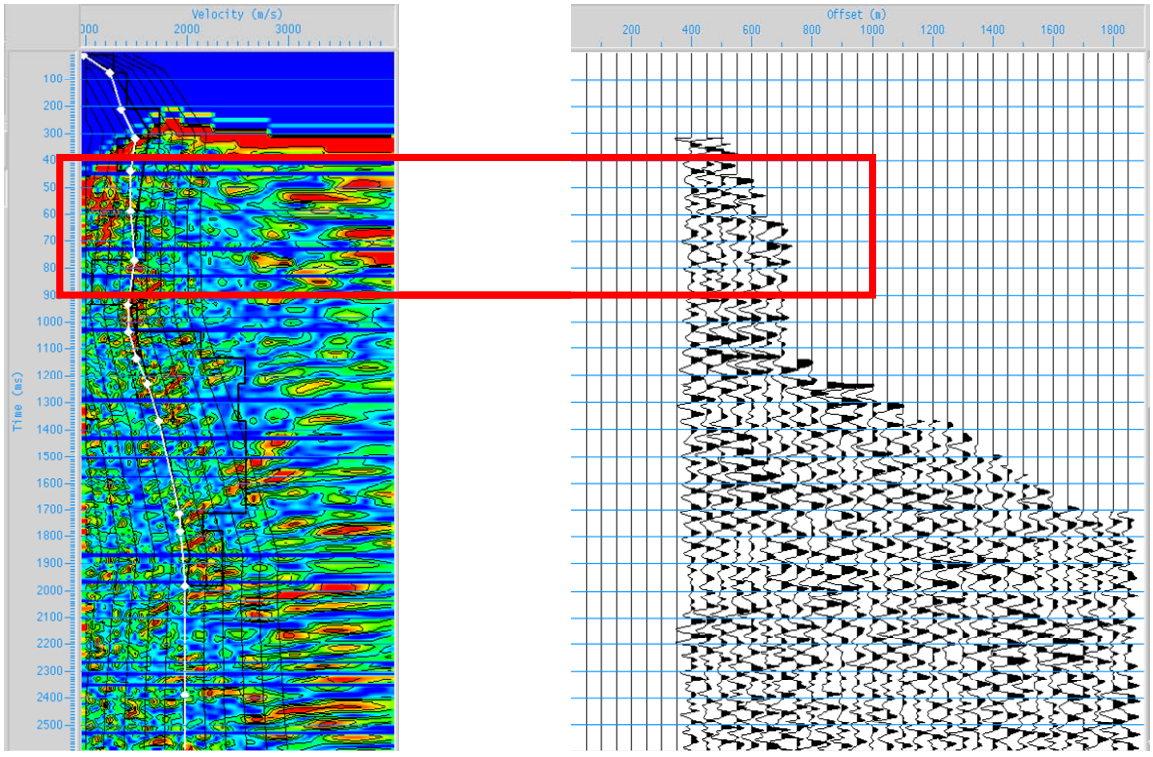

FIG. 7b. Radial component semblance-based velocity analysis. Super-ACP gather is on the left.

Statics

P-P shot and receiver statics have been calculated using GLI3D (Figure 8). It is difficult, if not impossible, to calculate *P-S* receiver statics, due to large lateral variations in the near-surface shear-velocity field. So, a receiver stack is created using *P-P* shot statics, *P-P* receiver statics scaled by a constant V_P/V_S ratio, and either a *P-S* velocity function from velocity analysis, or derived from *P-P* velocities (Figure 9a). In an iterative process, horizon(s) can be interpreted on this receiver stack and after flattening, are used to derive non-surface-consistent receiver statics for the *P-S* data (Figure 9b). For this survey, the first round of *P-S* receiver hand-statics varies by +/-120 ms (Figure 10), which is unusually large. All radial component stacks shown in this report are considered to be preliminary, as the process of picking *P-S* receiver statics is not yet complete.

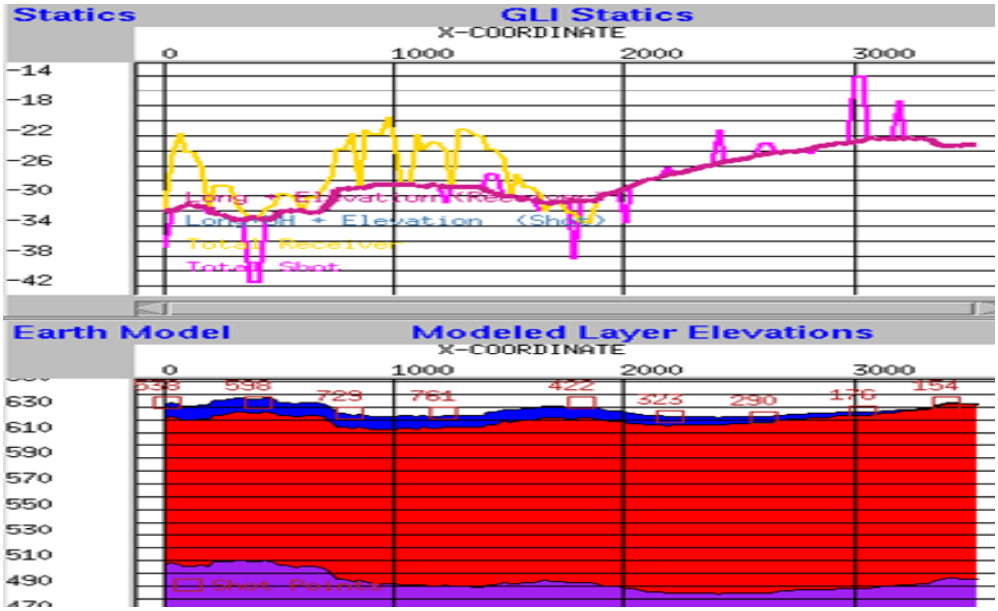

FIG. 8. Vertical component statics calculated in GLI3D. Total shot static is pink, total receiver static is yellow (top).

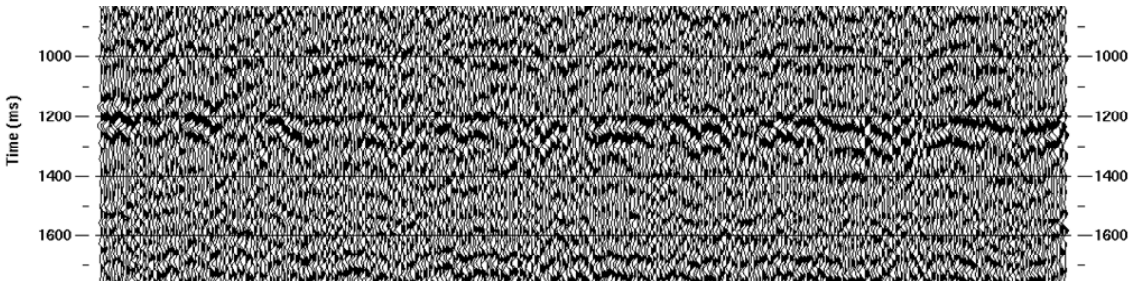

FIG. 9a. *P-S* receiver stack obtained using *P-P* shot statics and *P-P* receiver statics scaled by V_P/V_S = 2.3.

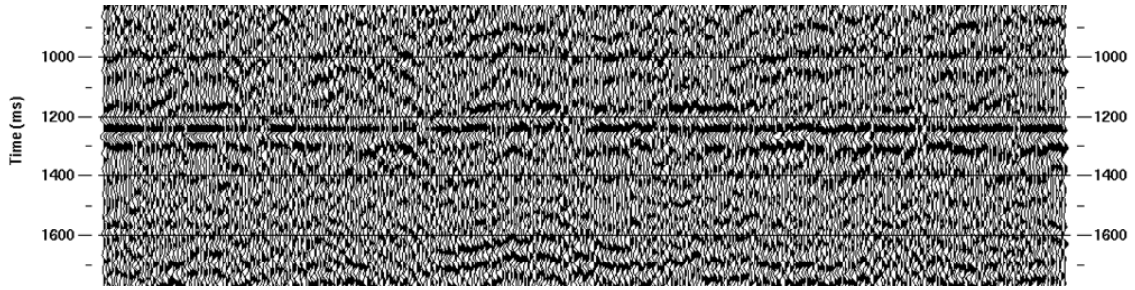

FIG. 9b. Figure 9a after one round of hand statics (cf. Figure 10).

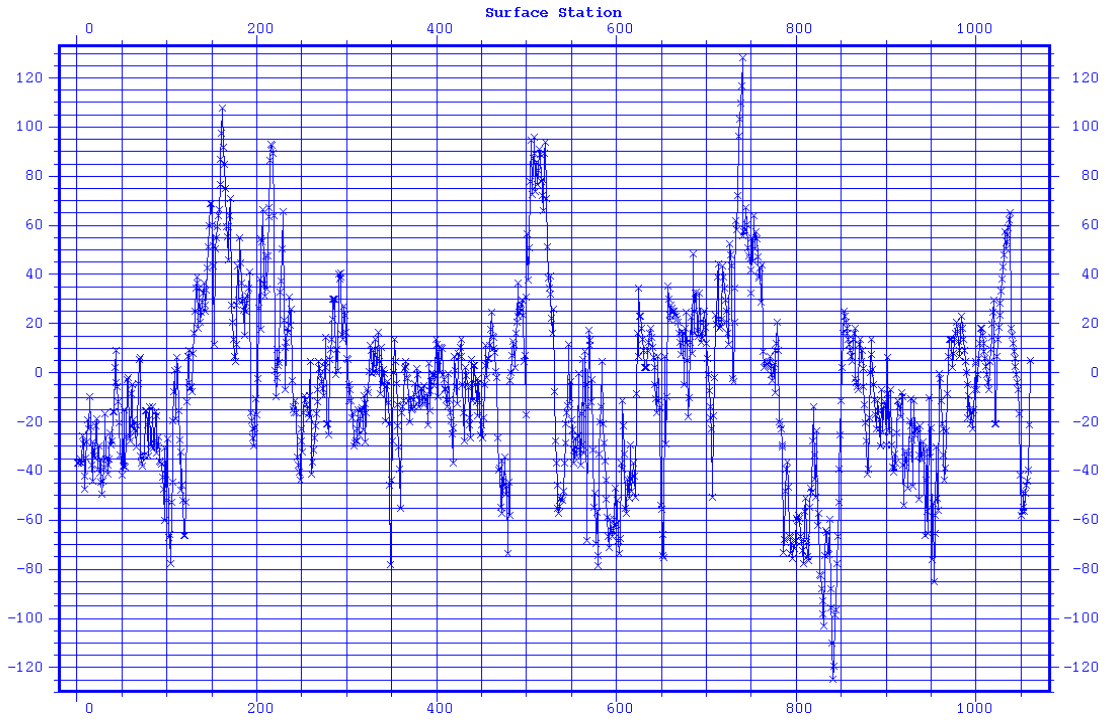

FIG. 10. Receiver statics used to obtain Figure 9b. Vertical scale is milliseconds.

RESULTS

Interpretation

P-P and *P-S* synthetics have been generated using the SYNGRAM program for well 11-17. A composite suite of well logs was created, with formation tops copied from 12-17. All logs were median-filtered with a three-point filter in LOGEDIT prior to importation into SYNGRAM. Constant-phase bandpass wavelets were created in WAVELETED, with frequency bands matching the bandpass filter used for the seismic displays (*P-P* = 10-15-90-110, *P-S* = 15-20-30-45; Figure 11). Figure 12 shows the synthetics overlain on the *P-P* (inline 28) and *P-S* (inline 30) migrated sections.

There is a good match between the synthetics and the seismic sections, which is very encouraging for future work. Figure 13 shows a comparison between *P-P* and *P-S* inlines, tied at crossline 76. The *P-S* inline has been stretched to *P-P* time based on the synthetic results. The best match between *P-P* and *P-S* reflections should be achieved in the 300-600 ms *P-P* time range.

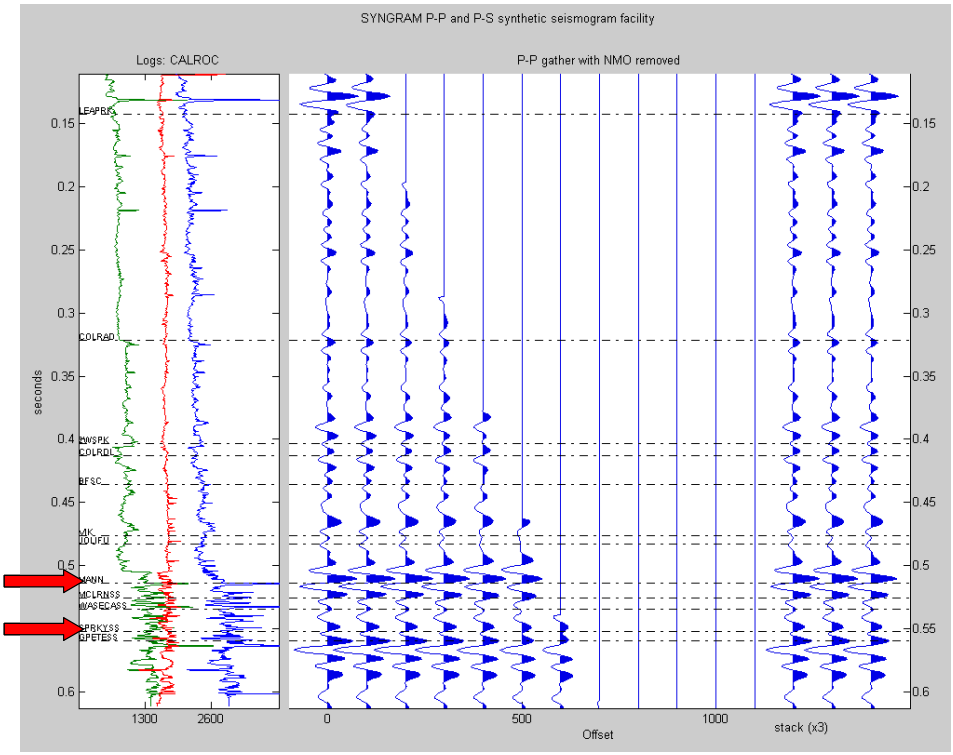

FIG. 11a. *P-P* synthetic for well 11-17. Arrows indicate top of Mannville Group (Colony member) and Sparky Formation (bottom). Logs are: *S*-velocity (green), density (red), *P*-velocity (blue).

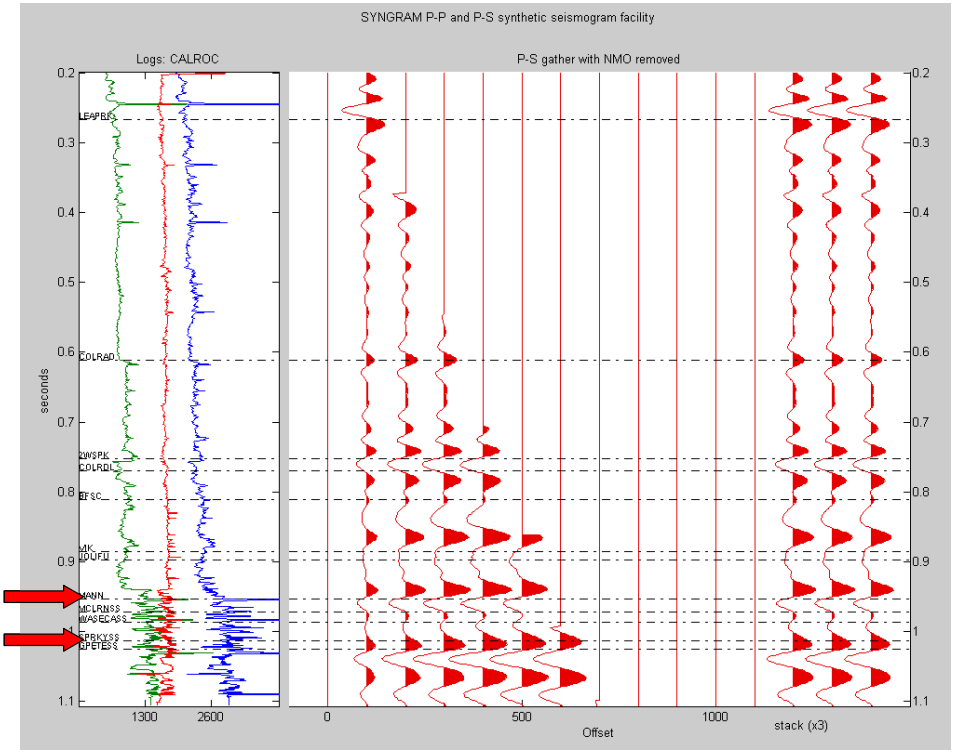

FIG. 11b. *P-S* synthetic for well 11-17. Arrows indicate top of Mannville Group (Colony member) and Sparky Formation (bottom). Logs are: *S*-velocity (green), density (red), *P*-velocity (blue).

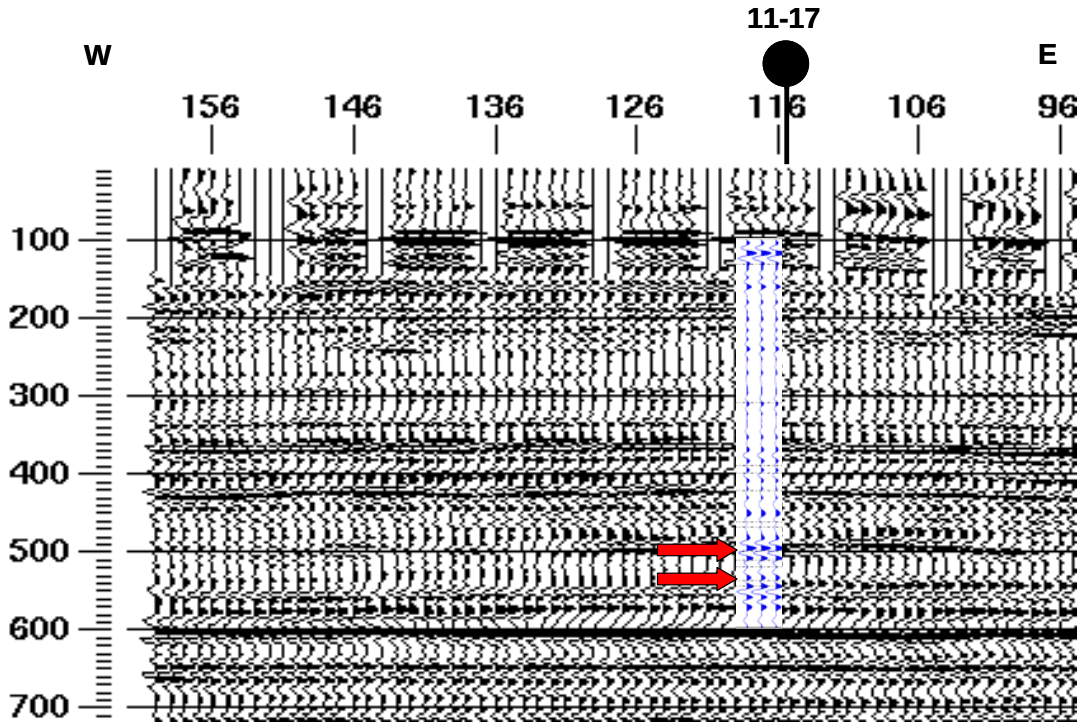

FIG. 12a. Portion of migrated *P-P* inline 28 with 11-17 synthetic (cf. Figure 11) projected onto the section along a Colony sand channel trend. Arrows indicate top of Mannville Group (Colony member) and Sparky Formation (bottom). Vertical scale is milliseconds.

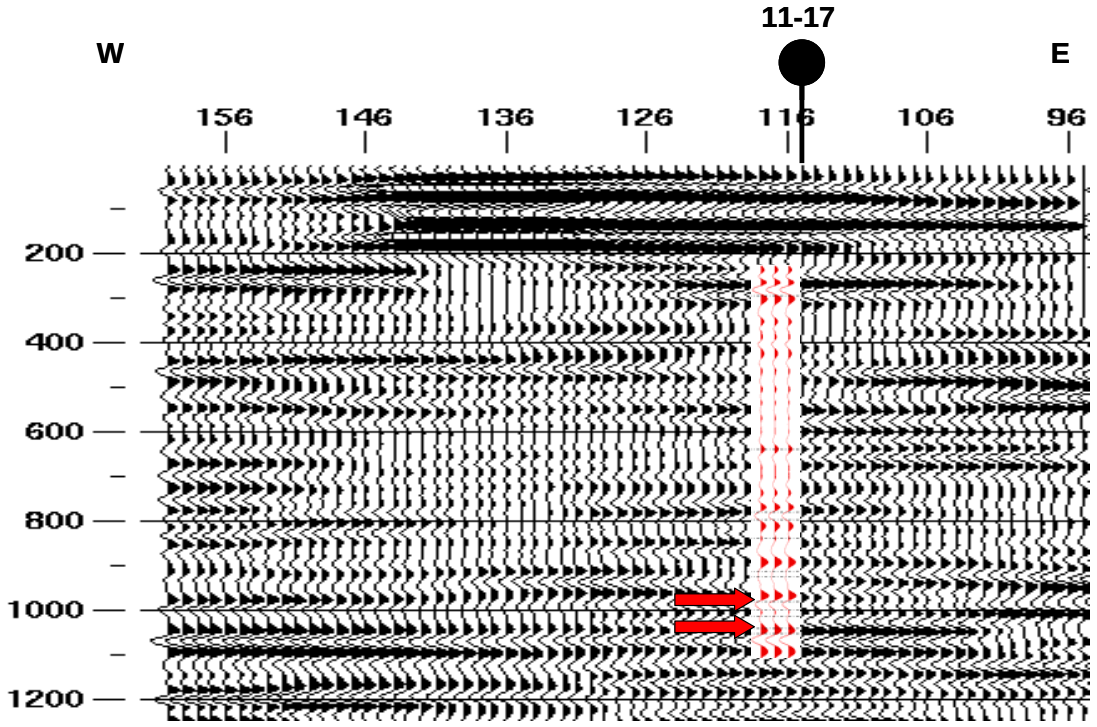

FIG. 12b. Portion of migrated *P-S* inline 30 with 11-17 synthetic (cf. Figure 11) projected onto the section along a Colony sand channel trend. Arrows indicate top of Mannville Group (Colony member) and Sparky Formation (bottom). Vertical scale is milliseconds.

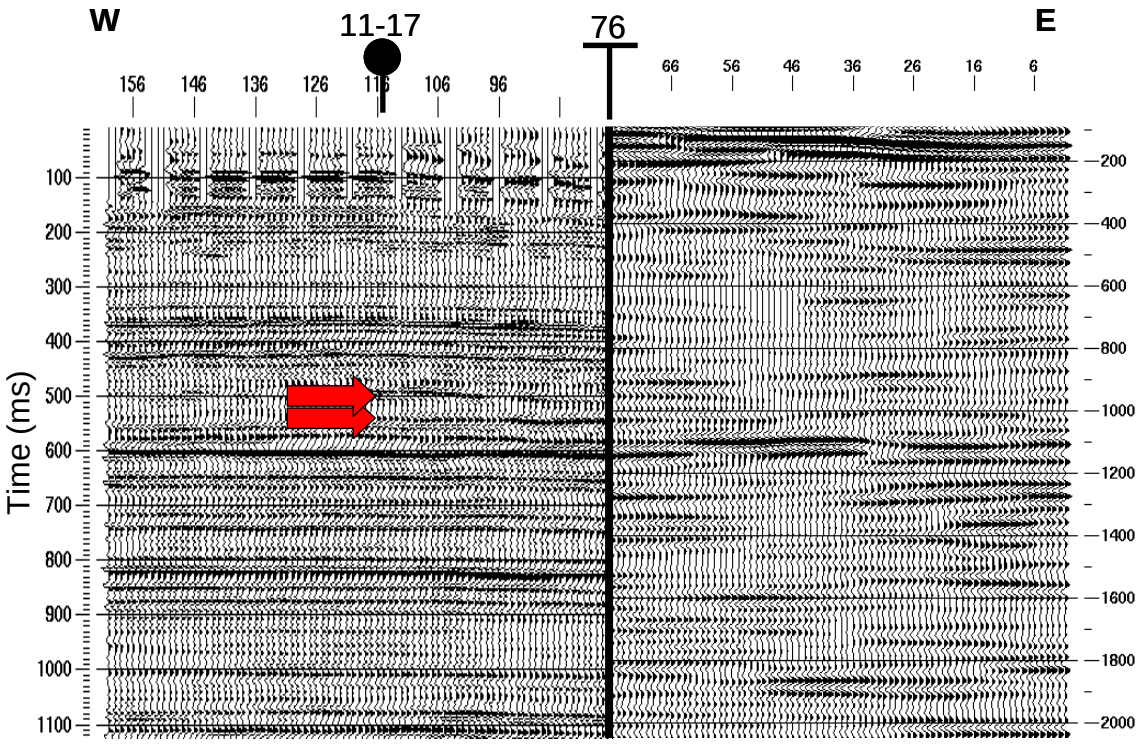

FIG. 13. Comparison of migrated *P-P* inline 28 (left) to migrated *P-S* inline 30 (right; stretched to *P-P* time based on synthetics shown in Figures 11 and 12). Arrows indicate top of Mannville Group (Colony member) and Sparky Formation (bottom).

Time slices

Figure 14 shows amplitude maps for two time-slices, 4 ms apart, through the *P-P* volume. An amplitude anomaly can be seen on both time-slices, which follows the well locations closely. Time-slices 2 ms above Figure 14a and 2 ms below Figure 14b show some channel-like features, but not as clearly.

The equivalent time-slices (6 ms apart) from the *P-S* volume are shown in Figure 15. The interpretation is less obvious in this case. The wormy character of these maps may be related to initial hand-picked *P-S* receiver statics. Hopefully, an improved statics solution will result in a more interpretable *P-S* volume.

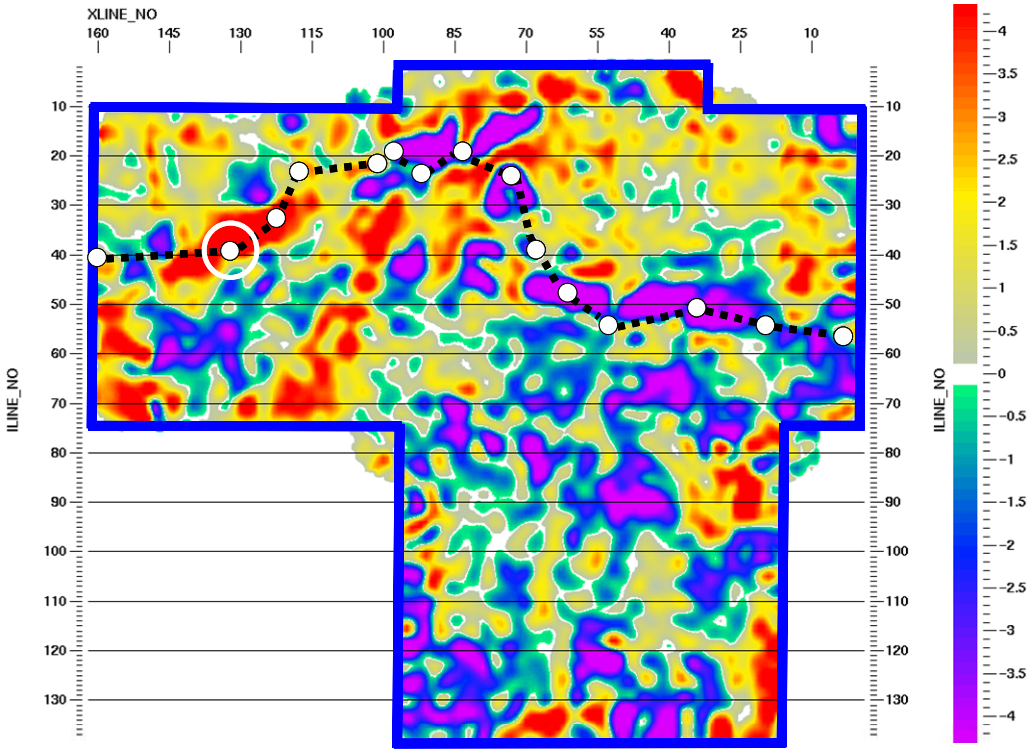

FIG. 14a. *P-P* volume; Time-slice near top of target zone. Dashed line and circles (white) show location of wells along a Colony member sand channel. Circled well is 11-17.

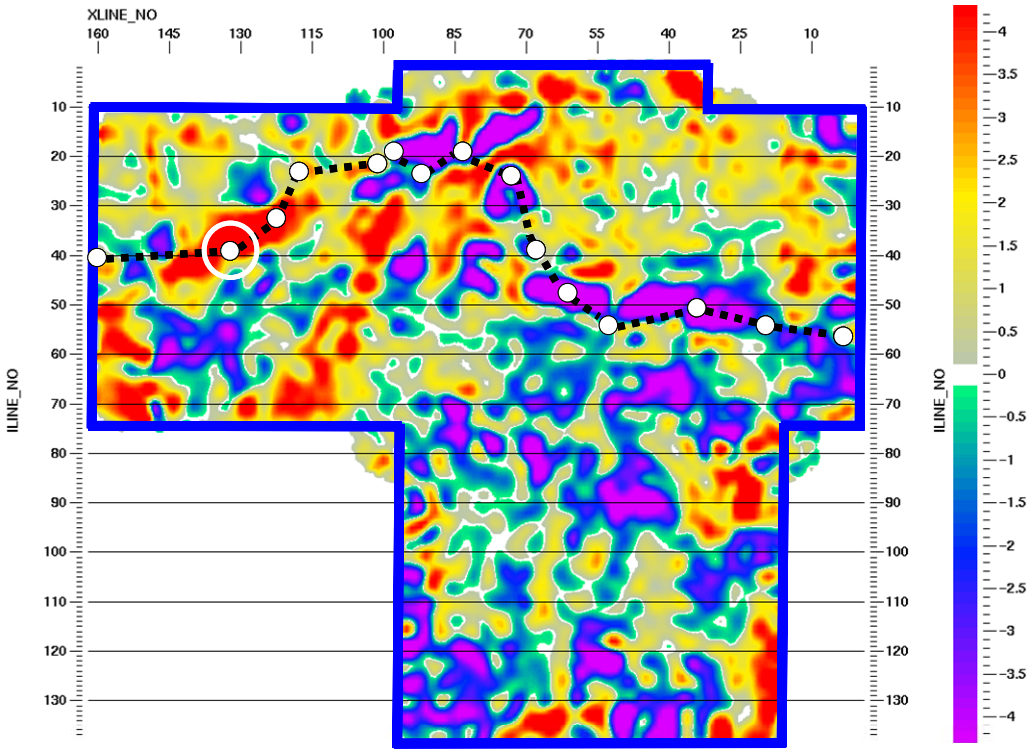

FIG. 14b. *P-P* volume; Time-slice 4 ms below Figure 14a.

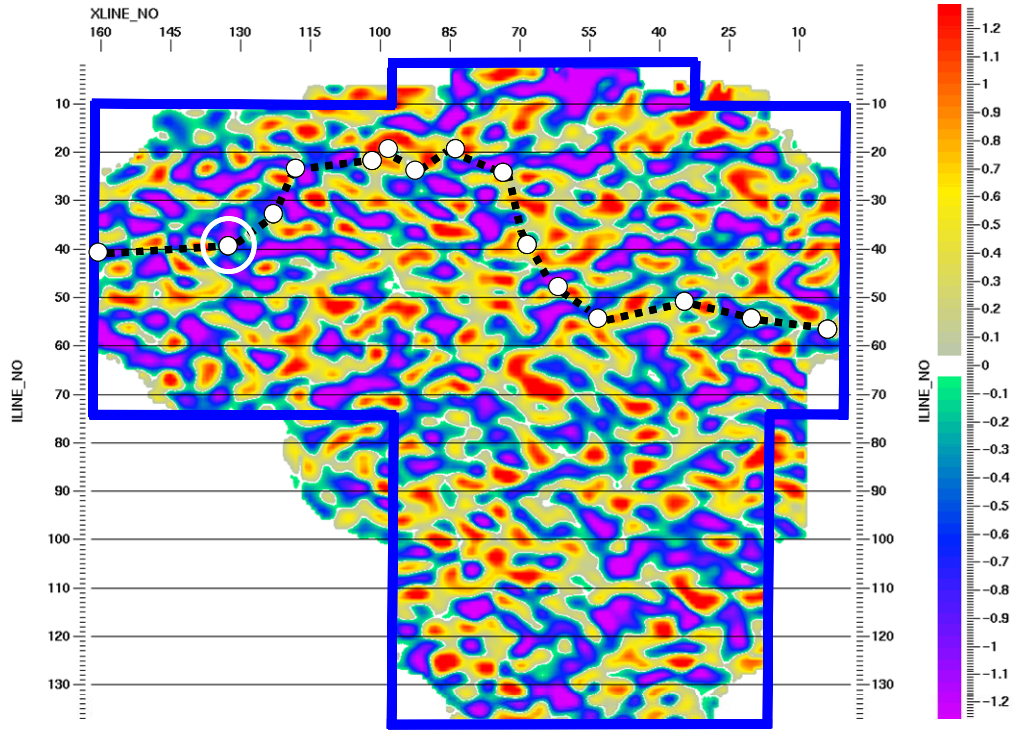

FIG. 15a. *P-S* volume; Time-slice near top of target zone. Dashed line and circles (white) show location of wells along a Colony member sand channel. Circled well is 11-17.

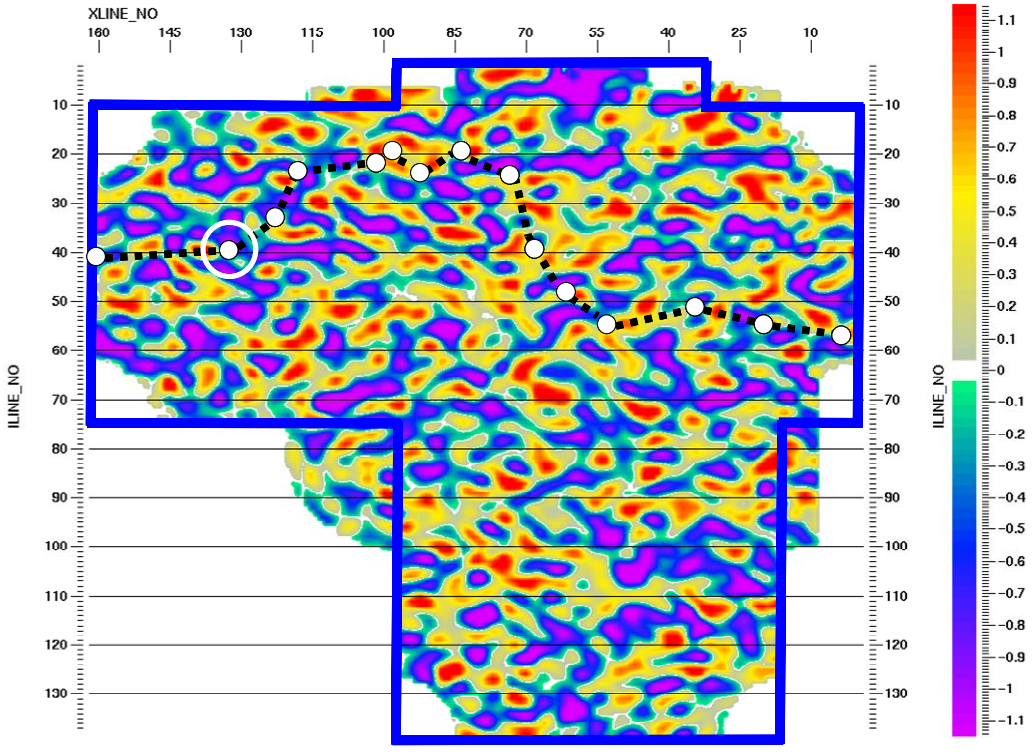

FIG. 15b. *P-S* volume; Time-slice 6 ms below Figure 15a.

DISCUSSION AND FUTURE WORK

The Manitou Lake 3C-3D survey has been processed to a final migrated *P-P* volume and a preliminary migrated *P-S* volume. Initial *P-S* results are promising, but reflection continuity is poor, especially on the cross-lines. Processing is ongoing, with an emphasis on noise reduction and *P-S* receiver statics. Source noise at near-offsets and aliased noise are both issues with the *P-S* data. We also suspect the radial component contains *P-P* energy, and plan to process the *P-S* data using *P-P* processing flows and parameters in order to test this. A re-examination of the component-rotation step may be warranted.

Preliminary interpretation results are encouraging, as the migrated volumes compare well to synthetic seismograms and to each other. *P-P* time-slices through the Colony sand member show an amplitude anomaly that closely follows surface well locations. Time-slices through the *P-S* volume are less promising, but it is hoped that improvements will be seen in the final volume.

Following completion of radial component processing, this survey is a good candidate for future AVO, interpretation, and joint-inversion projects.

ACKNOWLEDGEMENTS

We would like to Calroc Energy Inc. for providing this dataset to CREWES, Landmark Graphics Corporation and Veritas Hampson-Russell (VHR) for the use of donated software (ProMAX and GLI3D respectively). We also would like to thank all CREWES sponsors and NSERC for funding.

REFERENCES

Lu, H., and Margrave, G. F., 1998, Reprocessing the Blackfoot 3C-3D seismic data: CREWES Research Report, **10**.

Lu, H., and Hall, K. W., 2003, Tutorial: Converted-wave (2D PS) processing: CREWES Research Report, **15**.

Royle, A. J., 2001, Exploitation of an oil field using AVO and post-stack rock property analysis methods: CREWES Research Report, 13.

Royle, A. J., 2002, Exploitation of and oil field using AVO and post-stack property analysis methods: 72nd Ann. Internat. Mtg., Soc. Expl. Geophys., Expanded Abstracts, **21**, 289-292.

Putnam, P.E. and Oliver, T.A. 1980, Statigraphic traps in channel sandstones in the Upper Mannville (Albian) and east-central Alberta: Bulletin of Canadian Petroleum Geology, **28**, 489-508.